# Plasmonic Resonances in Nanostructured Transparent Conducting Oxide Films

Jongbum Kim, Gururaj V. Naik, Naresh K. Emani, *Member, IEEE*, Urcan Guler, and Alexandra Boltasseva, *Member, IEEE*

*(Invited Paper)*

***Abstract*—Transparent conducting oxides (TCOs) are emerging as possible alternative constituent materials to replace noble metals such as silver and gold for low-loss plasmonic and metamaterial (MM) applications in the near infrared regime (NIR). The optical characteristics of TCOs have been studied to evaluate the functionalities and potential of these materials as metal substitutes in plasmonic and MM devices, even apart from their usual use as electrode materials. However, patterning TCOs at the nanoscale, which is necessary for plasmonic and MM devices, is not well studied. This paper investigates nanopatterning processes for TCOs, especially the liftoff technique with electron-beam lithography, and the realization of plasmonic nanostructures with TCOs. By employing the developed nanopatterning process, we fabricate 2-D-periodic arrays of TCO nanodisks and characterize the material's plasmonic properties to evaluate the performance of TCOs as metal substitutes. Light-induced collective oscillations of the free electrons in the TCOs (bulk plasmons) and localized surface plasmon resonances are observed in the wavelength range from 1.6 to 2.1 $\mu$m. Well-defined resonance peaks are observed, which can be dramatically tuned by varying the amount of dopant and by thermally annealing the TCO nanodisks in nitrogen gas ambient while maintaining the low-loss properties.**

***Index Terms*—Nanopatterning, plasmonics, transparent conductive oxides (TCOs).**

## I. Introduction

FOR plasmonic systems [1], [2], noble metals traditionally have been used as metallic components due to their ability to support collective oscillations of free electrons (plasmons) at optical frequencies. However, the performance of plasmonic devices has been severely limited by the large optical losses in noble metals in the near infrared regime (NIR) [3], [4]. Recently, many studies have been conducted to characterize the optical properties of various alternative plasmonic materials such as metal alloys [5]–[7], transition-metal nitrides [8]–[10], and heavily doped semiconductors [3], [11]–[14] in order to find materials that could outperform noble metals for plasmonic and metamaterial (MM) applications. Such low-loss plasmonic materials would aid in overcoming the limitations of practical applications for plasmonic and MM systems. Recent studies have demonstrated that transparent conducting oxides (TCOs) such as Al- and Ga-doped zinc oxide (AZO, GZO) and tin-doped indium oxide (ITO) are good candidates as plasmonic materials in the near infrared frequency range because they exhibit metallic behavior and have smaller material loss compared to those of silver and gold in the NIR [8], [11], [13]. In our previous work [3], [15], we performed detailed comparative study of different materials including TCOs for various plasmonic and metamaterial applications and established that TCOs could potentially outperform metals in certain MM devices. So far, there are a few demonstrations where TCOs have been used as plasmonic materials, such as in semiconductor plasmonic quantum dots [16]–[18], plasmonic modulators [19], and negative refraction in AZO/ZnO MMs [20]. In these demonstrations, TCO-based devices showed better performance compared to noble metal-based devices in terms of lower losses and tunability. In addition, there are many other applications such as epsilon-near-zero devices [15], [21], [22], plasmonic metasurfaces such as polarization-sensitive surfaces [23], [24], and plasmonic gas sensors [15], [25], [26], where TCOs can be better alternatives to noble metals. Here, we report on the tunable plasmonic resonances in a metasurface formed by TCO nanodisks.

TCOs have long been used in display technologies as electrode materials [27], [28] because of their transparency in the visible range and low electrical resistance. As plasmonic components, TCOs exhibit lower optical loss with small magnitudes of real permittivity compared to those parameters exhibited by noble metals. TCOs additionally offer great modulation and switching possibilities that can new generation of tunable plasmonic and MM devices. To exhibit plasmonic properties, TCOs must have a carrier concentration higher than $10^{20}$ cm$^{-3}$, which leads metal-like behavior in the NIR. Note that if the carrier concentration in the host semiconductor of the TCO does not reach this level, the material will function as a dielectric in the NIR. By careful control and optimization of the fabrication conditions such as dopant type, doping concentration, deposition temperature, and deposition pressure, one can fabricate TCOs that exhibit the critical optical properties suitable for plasmonic applications in the NIR. Our recent studies showed that while being plasmonic, TCOs can have losses four times smaller than that of silver in the NIR [3]. Those two factors (low loss and plasmonic properties) open new routes to designing and realizing

Manuscript received August 20, 2012; revised December 20, 2012; accepted December 20, 2012. Date of publication January 21, 2013; date of current version April 25, 2013. This work was supported by the ONR-MURI-grant–N00014-10-1-0942.

The authors are with the Department of Electrical and Computer Engineering, Purdue University, West Lafayette, IN 47907-2057 USA (e-mail: kim668@purdue.edu; gnaik@purdue.edu; emani@purdue.edu; uguler@purdue.edu; aeb@purdue.edu).

Color versions of one or more of the figures in this paper are available online at http://ieeexplore.ieee.org.

Digital Object Identifier 10.1109/JSTQE.2013.2238611

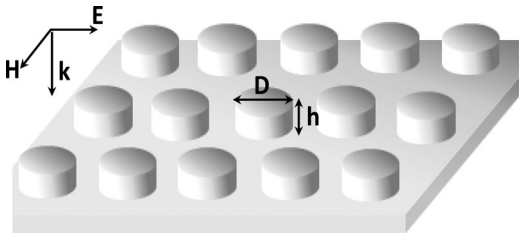


Fig. 1. Schematic view of a biperiodic array of TCO nanodisks and the definition of the relevant parameters.

plasmonic and optical MM devices with high performance at the technologically important near infrared wavelengths region including the telecommunication window around 1.55 $\mu$m.

The next important step along the path to replacing conventional metals with new materials is to develop the necessary nanopatterning techniques to make the new materials into designs and devices. This is a critical step because most plasmonic and MM devices are based on building blocks of nanostructured metals and dielectrics [29]–[31]. In our studies, we use a liftoff process with electron-beam lithography (EBL), a commonly used method to pattern nanoscale devices, to produce 2-D-periodic arrays of TCO nanodisks. The plasmonic properties of the TCO nanodisks are analyzed for a disk diameter range of 250–900 nm and for a constant disk height of 270 nm. We observe localized surface plasmon resonances (LSPRs) in the TCO nanodisk array at NIR frequencies, and we find that the LSPR wavelength and full-width at half-maximum of the resonance are remarkably sensitive both to the dimensions of the nanodisks and the doping density as well as to a subsequent thermal annealing treatment.

This paper is organized as follows. In Section II, we describe the procedure of the liftoff process and the restrictions on the deposition conditions set by the liftoff process. The optical properties of TCOs are strongly dependent on the deposition conditions, and thus, optimization is necessary to achieve the TCO properties required for plasmonic operation in the desired wavelength range. The TCO thin films are characterized with spectroscopic ellipsometry to retrieve their dielectric functions. Prism coupling experiments are performed to study the surface plasmon polariton (SPP) characteristics of the TCOs. In Section III, we analyze the plasmonic properties of the arrays of TCO nanodisks and demonstrate that the LSPR absorption of GZO nanodisks can be dynamically tuned across the NIR spectrum while maintaining the low-loss properties of the TCO by applying a thermal annealing treatment.

## II. Fabrication and Characterization

### A. Liftoff Process

To fabricate a 2-D array of TCO nanodisks as depicted schematically in Fig. 1, a silicon substrate was first spin-coated with a 1-$\mu$m-thick layer of positive electron-beam resist (ZEP 520 A) at 1000 r/min followed by the sample prebake at 180 °C for 2 min. The nanoscale pattern of cylindrical nanodisks was then exposed by EBL (Vistec VB6). The beam energy was 100 kV and the beam current was 1.012 nA. The base dose was maintained at 320 $\mu$C/cm$^2$. The exposed sample was developed in ZED-N50 (n-amyl acetate) for 1 min, and dipped in isopropyl alcohol for 30 s to rinse ZED-N50, and then dried in gaseous nitrogen. Prior to film deposition, a postbake was performed at 200 °C for 30 s. We deposited TCO films by pulsed laser deposition (PVD Products, Inc.) using a KrF excimer laser (Lambda Physik GmbH) operating at a wavelength of 248 nm for source material ablation.

The GZO, AZO, and ITO targets were purchased from the Kurt J. Lesker Corp. with purities of 99.99% or higher. The energy density of the laser beam at the target surface was maintained at 1.5 J/cm$^2$ [8]. A high oxygen partial pressure can etch the e-beam resist during the deposition process due to reaction with oxygen gas [32]. Thus, all the films were grown with an oxygen partial pressure of 0.2 mTorr (0.027 Pa) or lower. Since e-beam resist can become hard-baked from elevated substrate temperatures during a deposition process, the deposition temperature should be maintained as low as possible in order to facilitate the subsequent liftoff process. In our studies, the substrate temperature during TCO thin film deposition was optimized at 70 °C.

For the liftoff process, the sample deposited with a TCO film was dipped in ZDMAC (dimethylacetamide) for 10 min and sonicated for 1 min. Most of the e-beam resist was removed during this process, but small amounts of resist remained on the edges and sides of the nanostructures. In order to remove the residual e-beam resist, the sample was dipped in PRS 2000 stripper at 70 °C for 30 min and then dipped in acetone for 5 min for rinsing.

### B. Ellipsometric Characterization

The optical properties of the TCO films were characterized by spectroscopic ellipsometry (V-VASE, J. A. Woollam) in the spectral region from 350 to 2000 nm. The dielectric function of the film was retrieved by fitting a Drude–Lorentz oscillator model to the ellipsometry data. In semiconductors, conduction electrons have a nearly continuum of available states, so that their interaction with an electromagnetic field is well approximated by Drude theory, where conduction electrons are treated as a 3-D free-electron gas. The Lorentz oscillator model is used to describe the absorption of photons by valence electrons. An electron in valence band jumps to conduction band by absorbing a photon, resulting in optical loss [3]. The following equation describes the Drude–Lorentz oscillator model, where the second term comes from the Drude model and the third term represents the Lorentz oscillator. The retrieved model parameters are listed in Table I:

$$\varepsilon(\omega) = \varepsilon_\infty - \frac{\omega_p^2}{\omega(\omega + i\Gamma_p)} + \frac{f_1\omega_1^2}{\omega_1^2 - \omega^2 - i\omega\Gamma_1} \qquad (1)$$

where $\varepsilon_\infty$ is the background permittivity, $\omega_p$ is the unscreened plasma frequency, $\Gamma_p$ is the carrier relaxation rate, and $f_l$ is the strength of the Lorentz oscillator with center frequency $\omega_l$ and damping $\Gamma_l$.

Fig. 2 shows the optical properties of AZO, GZO, and ITO films deposited under conditions optimized for the liftoff

TABLE I
DRUDE–LORENTZ MODEL PARAMETERS FOR TCOS

| | AZO (2wt%) | GZO (6wt%) | ITO (10wt%) |
|---|---|---|---|
| $\varepsilon_\infty$ | 2.852 | 2.475 | 3.528 |
| $\omega_p$ (eV) | 1.512 | 1.927 | 1.780 |
| $\Gamma_p$ (eV) | 0.089 | 0.117 | 0.155 |
| $f_l$ | 0.596 | 0.866 | 0.388 |
| $\omega_l$ (eV) | 4.384 | 4.850 | 4.210 |
| $\Gamma_l$ (eV) | 0.078 | 0.029 | 0.092 |

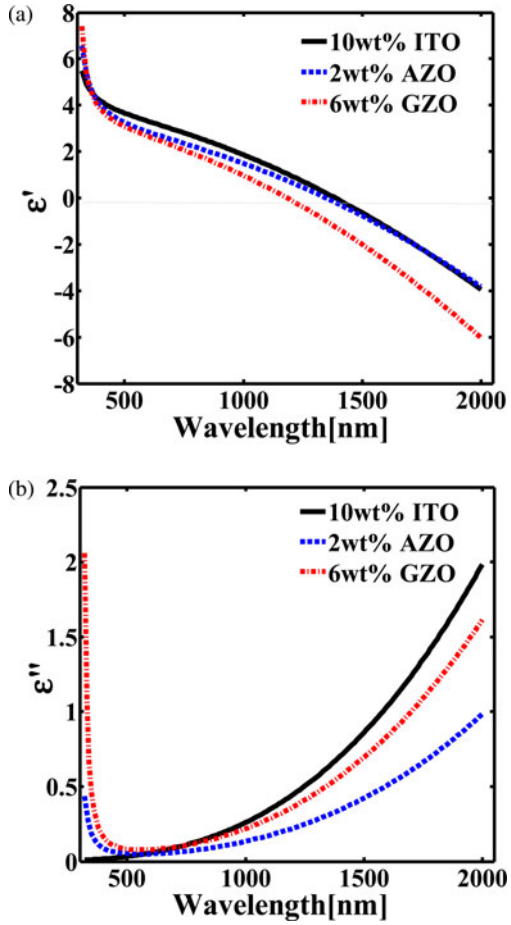


Fig. 2. Comparison of the optical properties of TCO films deposited under optimized conditions for the liftoff process. (a) Real part of the spectral dielectric function. (b) Imaginary part of the spectral dielectric function.

process. Notably, the crossover wavelengths of all the TCO films are below telecommunication wavelength of 1.55 $\mu$m. Compared to our previous study [8], the optical properties of these TCO films are improved in terms of their metallic behavior and optical losses. The AZO film offers the lowest optical loss, referring to the imaginary part of its permittivity. Note that GZO can provide a crossover wavelength as low as 1.2 $\mu$m, but the optical loss in GZO is higher than that in AZO. Under conditions optimized for the liftoff process, the ITO film has the highest loss and the largest crossover wavelength compared to AZO and GZO.

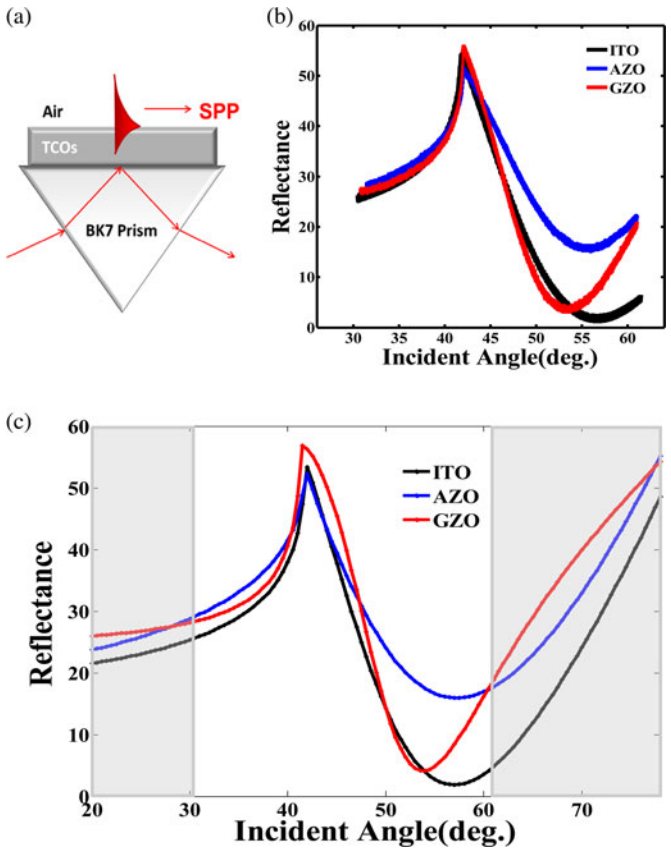


Fig. 3. (a) Schematic view of the experimental setup for SPP excitation in attenuated total reflection. (b) Reflectance curve versus incident angle of light with 1.55-$\mu$m wavelength for ITO, AZO, and GZO. (c) Simulation of reflectance curve versus incident angle of light with 1.55-$\mu$m wavelength for ITO, AZO, and GZO.

### C. Prism Coupling for SPP Measurements

SPPs are propagating charge-density waves on metal–dielectric interface that can be excited by attenuated total reflection of an incident electromagnetic wave [33]. In this study, SPP excitation on TCO films was used to verify the applicability of these materials for NIR plasmonic devices, especially at the telecommunication wavelength of 1.55 $\mu$m. We used a prism coupler (Metricon 2010/M) and implemented a Kretschmann–Raether configuration for SPP coupling (see Fig. 3). The TCO thin films were directly deposited on BK7 glass coupling prisms ($n = 1.501$), and the thicknesses of AZO, GZO, and ITO were 154, 147, and 139 nm, respectively.

Avsp beam of TM-polarized, monochromatic laser at a wavelength of 1.55 $\mu$m was used to illuminate the sample through the input facet of the 45° BK7 glass coupling prism. While rotating the sample with respect to the laser beam, the far-field reflectance was measured with a detector. This provided a measurement of the reflected intensity for a range of internal angles from 30° to 62°. Theoretically, SPPs at a TCO-air interface are expected in wavelength region where the real part of the TCO permittivity ($\varepsilon'_{\mathrm{TCO}}$) is less than $-1$.

The experimental observation of broad SPP resonances in ITO films was previously reported in [34], [35]. Those reports demonstrated a thickness-dependent SPP on ITO thin films.

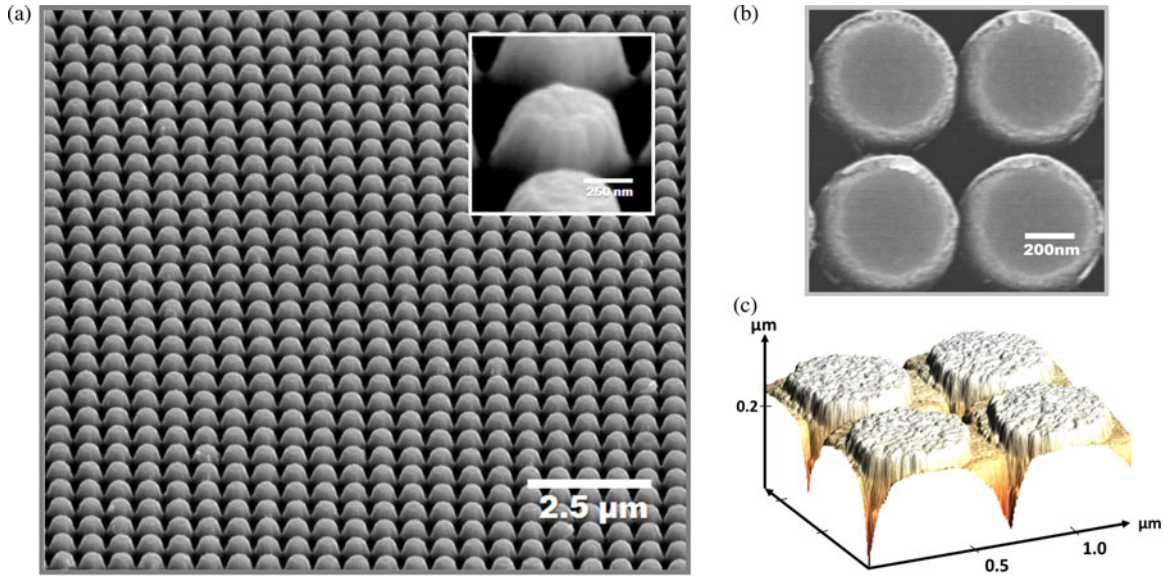


Fig. 4. (a) 54° tilted SEM image of an array of GZO nanodisks with a mean diameter $D = 500$ nm and height $h = 270$ nm. (Inset) SEM image of GZO nanodisks at high magnification. (b) Top-down view of the nanodisks showing nearly circular shapes. (c) AFM scan of the GZO nanodisks.

AZO was previously reported to be incapable of supporting SPPs at 1.55 $\mu$m because of its smaller plasma frequency. However, the AZO films in this and our previous work [8] are optimized for large plasma frequencies at 1.55 $\mu$m. The experimental data from the prism coupling reflectance measurements clearly show the SPP existence on AZO films at a wavelength of 1.55 $\mu$m [see Fig. 3(b)]. The reflectance measurements from the prism coupler were verified using analytic calculations. Fig. 3(c) shows the calculated reflectance values for AZO, GZO, and ITO thin films. The dip in reflectance occurring around 50–60° corresponds to the excitation of SPPs on these films.

## III. Arrays of Nanodisks

### A. Structural Characterization

Plasmonic structures such as nanodisks of noble metals have been studied extensively [36], [37] since their strong resonant interaction with light is useful in many applications such as sensors. In this paper, a polarization-independent design consisting of a periodic 2-D array of nanodisks is used to study the plasmonic properties of TCO nanostructures and to compare those properties to previous studies with noble metals. As shown in Fig. 4, we fabricated a square array of 270-nm-thick GZO nanodisks with a spacing of 100 nm between adjacent nanodisks. The nanodisk diameter was varied from 250 to 900 nm over a number of samples. In order to make the LSPR structures covering much of the NIR spectrum (including the telecommunications wavelengths), we fabricated the nanodisk array with GZO because it has higher plasma frequency compared to other TCOs. The scanning electron microscope (SEM) image in Fig. 4(a) shows the uniformity of the nanopatterned arrays in a relatively large area of nanoscale devices. The shape of nanodisk is almost perfectly circular shown in Fig. 4(b). It is important to note that the deposition of the GZO layer on a patterned e-beam resist and its subsequent liftoff produces non-vertical side walls. As a result, the cross section of the nanodisk represents a trapezoidal shape [see the inset of Fig. 4(a)]. For morphological analysis, we scanned the sample with an atomic force microscope (Veeco Dimension 3100 AFM) to check the roughness of the nanodisk top surface. We used standard Si probe tips with the atomic force microscopy (AFM) in tapping mode. The resolutions of our AFM scans were not sufficient to accurately investigate the full depths of the narrow gaps between nanodisks. Hence, it is difficult to see the cross-sectional dimension of the nanodisks from the AFM image shown in Fig. 4(c). The root-mean-squared (RMS) roughness of the tops of the patterned nanodisks was about 6–8 nm. For as-deposited GZO thin films without any patterning processing, the RMS roughness is 5–7 nm. We can, therefore, confirm that the liftoff process does not significantly affect the surface morphology of the developed TCO material.

### B. Optical Characterization

The transmission spectra of the nanodisk arrays are obtained using a V-VASE spectroscopic ellipsometer with a normally incident TE wave. The measurement is performed in the wavelength range from 1.1 to 2.4 $\mu$m (see Fig. 5). Note that absorption below 1.2 $\mu$m corresponds to phonon-assisted interband optical absorption in the silicon substrate. The LSPR wavelength and intensity depend on the size, shape, and properties of the nanostructured array [38]–[40].

In our studies, we investigate the effects of disk size and doping density on the LSPR properties. The transmission spectra reveal well-defined LSPR peaks, and the positions of these peaks depend on both the disk size and the doping density. As the disk diameter increases (see Fig. 5), the resonance red shifts and becomes stronger. However, the transmission peak broadens as the disk diameter increases. This is due to the fact that the disks begin to support higher order plasmonic modes that start to overlap as the disk size increases [41], [42]. The experimental trends are

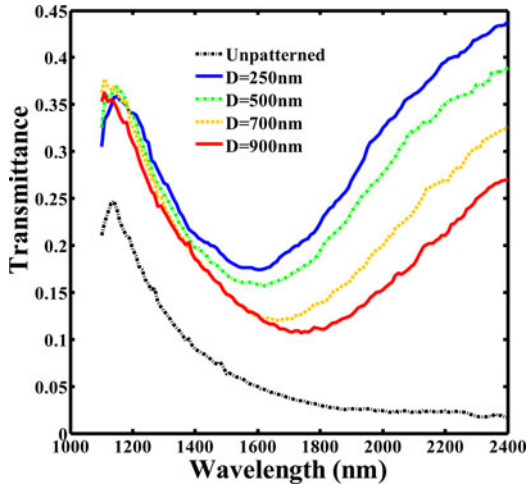


Fig. 5. Transmittance spectra for GZO nanodisk array samples and unpatterned GZO thin film on Si substrates with different nanodisk diameters.

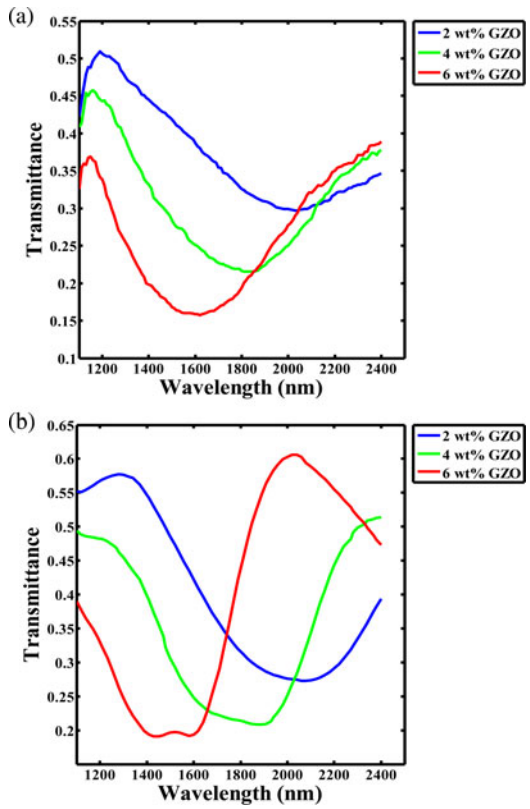


Fig. 6. (a) Measured transmittance spectra for the GZO nanodisk arrays (disk diameter of 500 nm) with different doping ratios in the GZO material. (b) Simulation results of transmittance spectra for GZO nanodisk arrays using different dielectric functions for films with different doping concentrations.

verified by simulations with finite-element-method-based commercial software, Comsol Multiphysics. Trapezoidal nanodisk structures are used with the optical properties obtained from thin films co-deposited with the nanostructures. Fig. 6(b) shows the simulation results for the GZO nanodisks with varying doping densities. Although some minor mismatch due to fabrication imperfections exists, numerical results are in good agreement with the experiments. In our previous study [8], we reported the change of plasma frequency and optical loss depending on doping density. As the doping density of GZO increases [see Fig. 6(a)], the films exhibit higher plasma frequency, and hence, the resonance shifts to shorter wavelengths. The optical loss of GZO is increased as reducing the doping density. The broadening of resonance peak corresponds to the increase of optical loss. In terms of the tunability of the LSPR wavelength, the peak shift arising from the change in doping density is much stronger than that caused by the nanodisk geometry.

### *C. Thermal Annealing*

Thermal treatments on TCO films have been well studied in transparent electrode research in order to enhance the crystallinity and hence, the transparency of TCO films [43]–[45]. The effect of thermal annealing on a TCO film is strongly dependent on the temperature and the type of ambient gas. In order to characterize the effect of thermal annealing on plasmonic properties, we first investigated the annealing effect on the optical properties of TCOs with respect to two aspects: carrier concentration and optical loss. The GZO nanodisk sample was annealed up to 350 °C for an hour in nitrogen ambient to observe the effect of the annealing gas on the optical loss.

The resulting transmittance spectra in Fig. 7(a) show that the thermal treatment can dramatically tune the LSPR peak to longer wavelengths due to reductions in the carrier concentration. Post-deposition anneal offers a way to control the LSPR properties through a postfabrication treatment without any changes in optical loss of TCOs. This allows for flexibility in the design and optimization of the LSPR nanostructure. In Fig. 7(b), we plot the Drude damping coefficient and crossover frequency $\omega_c$ as functions of the annealing temperature with either a nitrogen or oxygen ambient. The Drude damping coefficient is indicative of the optical losses occurring in the material, and the crossover frequency $\omega_c$ is defined as the frequency at which the real part of permittivity of the material crosses zero. Since $\omega_c$ is directly proportional to the plasma frequency $\omega_p$, and $\omega_p$ is proportional to the square of the carrier concentration, the plot in Fig. 7(b) in essence shows the carrier concentration trend with respect to the annealing temperature.

We see in the figure that the carrier concentration decreases with increasing annealing temperature for both types of ambient gas. The optical loss strongly increases after annealing in oxygen ambient, while the optical loss remains the same after annealing in the nitrogen ambient.

The morphological and structural modifications incurred by the annealing treatment have already been examined in the case of noble metals [36], [46]. In those studies, the goal was to improve quality of the LSPR properties through an annealing treatment. We carry out similar studies on TCOs in this paper. The SEM image in Fig. 7(c) shows that there are no substantial changes in the nanodisk shape or morphology for annealing temperatures up to 350 °C. Given that TCOs are ceramics, we would expect this trend to continue for higher temperatures as well. In contrast, noble metal nanostructures are known to deform when annealed at such temperatures.

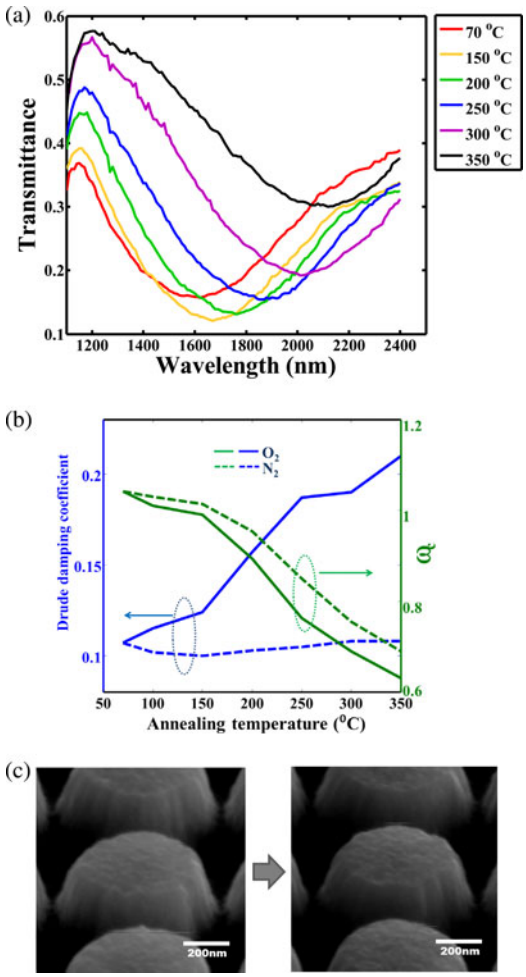


Fig. 7. (a) Transmittance spectra for GZO nanodisk arrays with different thermal annealing temperatures in a nitrogen ambient. (b) Drude damping coefficient and crossover frequency $\omega_c$ versus annealing temperature in either oxygen or nitrogen ambient gas. (c) SEM image of nanodisk before and after thermal treatment.

## IV. Conclusion

In conclusion, TCOs are good alternatives to noble metals for plasmonic applications in the NIR. We observed that thin films of AZO, GZO, and ITO can support SPPs at telecommunication wavelengths. We showed that standard nanofabrication techniques may be used to pattern these TCO films. When patterned, these materials exhibit LSPR properties similar to gold and silver nanostructures. The resonance properties strongly depend on the properties of the film such as carrier concentration. Thermal annealing in different gases altered the resonance by changing the carrier concentration in these films. At the same time, in contrast to noble metals, no significant changes in morphology, surface roughness, and grain structure were observed in GZO nanodisks after annealing. The effect of the carrier concentration via annealing can be used for postfabrication tuning of the properties of TCO devices. Such tunability of the TCO properties could be used to tailor the optical resonance for various plasmonic applications and enable a new generation of controllable, switchable devices.

## References

[1] W. L. Barnes, A. Dereux, and T. W. Ebbesen, "Surface plasmon subwavelength optics," *Nature*, vol. 424, pp. 824–830, 2003.
[2] S. Lal, S. Link, and N. J. Halas, "Nano-optics from sensing to waveguiding," *Nature Photon.*, vol. 1, pp. 641–648, 2007.
[3] P. R. West, S. Ishii, G. V. Naik, N. K. Emani, V. M. Shalaev, and A. Boltasseva, "Searching for better plasmonic materials," *Laser Photon. Rev.*, vol. 4, pp. 795–808, 2010.
[4] A. Boltasseva and H. A. Atwater, "Low-loss plasmonic metamaterials," *Science*, vol. 331, pp. 290–291, 2011.
[5] D. A. Bobb, G. Zhu, M. Mayy, A. V. Gavrilenko, P. Mead, V. I. Gavrilenko, and M. A. Noginov, "Engineering of low-loss metal for nanoplasmonic and metamaterials applications," *Appl. Phys. Lett.*, vol. 95, pp. 151102–151103, 2009.
[6] M. Blaber, M. Arnold, and M. Ford, "Optical properties of intermetallic compounds from first principles calculations: A search for the ideal plasmonic material," *J. Phys.: Condensed Matter*, vol. 21, p. 144211, 2009.
[7] M. G. Blaber, M. D. Arnold, and M. J. Ford, "A review of the optical properties of alloys and intermetallics for plasmonics," *J. Phys.: Condensed Matter*, vol. 22, p. 143201, 2010.
[8] G. V. Naik, J. Kim, and A. Boltasseva, "Oxides and nitrides as alternative plasmonic materials in the optical range," *Opt. Mater. Exp.*, vol. 1, pp. 1090–1099, 2011.
[9] G. V. Naik, J. L. Schroeder, X. Ni, A. V. Kildishev, T. D. Sands, and A. Boltasseva, "Titanium nitride as a plasmonic material for visible and near-infrared wavelengths," *Opt. Mater. Exp.*, vol. 2, pp. 478–489, 2012.
[10] U. Guler, G. Naik, A. Boltasseva, V. Shalaev, and A. Kildishev, "Nitrides as alternative materials for localized surface plasmon applications," presented at the Frontiers in Optics, Rochester, NY, 2012.
[11] S. Franzen, "Surface plasmon polaritons and screened plasma absorption in indium tin oxide compared to silver and gold," *J. Phys. Chem. C*, vol. 112, pp. 6027–6032, 2008.
[12] C. Rhodes, S. Franzen, J. P. Maria, M. Losego, D. N. Leonard, B. Laughlin, G. Duscher, and S. Weibel, "Surface plasmon resonance in conducting metal oxides," *J. Appl. Phys.*, vol. 100, p. 054905, 2006.
[13] G. V. Naik and A. Boltasseva, "Semiconductors for plasmonics and metamaterials," *Physica Status Solidi-Rapid Res. Lett.*, vol. 4, pp. 295–297, 2010.
[14] M. Noginov, L. Gu, J. Livenere, G. Zhu, A. Pradhan, R. Mundle, M. Bahoura, Y. A. Barnakov, and V. Podolskiy, "Transparent conductive oxides: Plasmonic materials for telecom wavelengths," *Appl. Phys. Lett.*, vol. 99, p. 021101, 2011.
[15] G. V. Naik and A. Boltasseva, "A comparative study of semiconductor-based plasmonic metamaterials," *Metamaterials*, vol. 5, pp. 1–7, 2011.
[16] G. Garcia, R. Buonsanti, E. L. Runnerstrom, R. J. Mendelsberg, A. Llordes, A. Anders, T. J. Richardson, and D. J. Milliron, "Dynamically modulating the surface plasmon resonance of doped semiconductor nanocrystals," *Nano Lett.*, vol. 11, pp. 4415–4420, 2011.
[17] R. Buonsanti, A. Llordes, S. Aloni, B. A. Helms, and D. J. Milliron, "Tunable infrared absorption and visible transparency of colloidal aluminum-doped zinc oxide nanocrystals," *Nano Lett.*, vol. 11, pp. 4706–4710, 2011.
[18] S. Q. Li, P. Guo, L. Zhang, W. Zhou, T. W. Odom, T. Seideman, J. B. Ketterson, and R. P. H. Chang, "Infrared plasmonics with indium-tin-oxide nanorod arrays," *ACS Nano*, vol. 5, pp. 9161–9170, 2011.
[19] A. Melikyan, N. Lindenmann, S. Walheim, P. M. Leufke, S. Ulrich, J. Ye, P. Vincze, H. Hahn, T. Schimmel, C. Koos, W. Freude, and J. Leuthold, "Surface plasmon polariton absorption modulator," *Opt. Exp.*, vol. 19, pp. 8855–8869, 2011.
[20] G. V. Naik, J. Liu, A. V. Kildishev, V. M. Shalaev, and A. Boltasseva, "Demonstration of Al: ZnO as a plasmonic component for near-infrared metamaterials," *Proc. Nat. Acad. Sci.*, vol. 109, pp. 8834–8838, 2012.
[21] M. Silveirinha and N. Engheta, "Tunneling of electromagnetic energy through subwavelength channels and bends using $\varepsilon$-near-zero materials," *Phys. Rev. Lett.*, vol. 97, p. 157403, 2006.
[22] N. Engheta, "Circuits with light at nanoscales: Optical nanocircuits inspired by metamaterials," *Science*, vol. 317, pp. 1698–1702, 2007.
[23] Y. Zhao and A. Alù, "Manipulating light polarization with ultrathin plasmonic metasurfaces," *Phys. Rev. B*, vol. 84, p. 205428, 2011.
[24] Y. Zhao, M. Belkin, and A. Alù, "Twisted optical metamaterials for planarized ultrathin broadband circular polarizers," *Nature Commun.*, vol. 3, p. 870, 2012.
[25] S. K. Mishra, D. Kumari, and B. D. Gupta, "Surface plasmon resonance based fiber optic ammonia gas sensor using ITO and polyaniline," *Sens. Actuators B: Chem.*, vol. 171/172, pp. 976–983, 2012.

[26] S. K. Mishra and B. D. Gupta, "Surface plasmon resonance-based fiber-optic hydrogen gas sensor utilizing indium–tin oxide (ITO) thin films," *Plasmonics*, vol. 7, pp. 627–632, 2012.
[27] D. S. Ginley and C. Bright, "Transparent conducting oxides," *MRS Bull.*, vol. 25, pp. 15–18, 2000.
[28] T. Minami, "New n-type transparent conducting oxides," *MRS Bull.*, vol. 25, pp. 38–44, 2000.
[29] S. Link and M. A. El-Sayed, "Spectral properties and relaxation dynamics of surface plasmon electronic oscillations in gold and silver nanodots and nanorods," *J. Phys. Chem. B*, vol. 103, pp. 8410–8426, 1999.
[30] N. Liu, M. L. Tang, M. Hentschel, H. Giessen, and A. P. Alivisatos, "Nanoantenna-enhanced gas sensing in a single tailored nanofocus," *Nature Mater.*, vol. 10, pp. 631–636, 2011.
[31] V. M. Shalaev, "Optical negative-index metamaterials," *Nature Photon.*, vol. 1, pp. 41–48, 2007.
[32] G. Taylor and T. Wolf, "Oxygen plasma removal of thin polymer films," *Polymer Eng. Sci.*, vol. 20, pp. 1087–1092, 1980.
[33] B. E. Sernelius and B. Sernelius, *Surface Modes in Physics*. New York, USA: Wiley, 2001.
[34] C. Rhodes, M. Cerruti, A. Efremenko, M. Losego, D. Aspnes, J. P. Maria, and S. Franzen, "Dependence of plasmon polaritons on the thickness of indium tin oxide thin films," *J. Appl. Phys.*, vol. 103, p. 093108, 2008.
[35] L. Dominici, F. Michelotti, T. M. Brown, A. Reale, and A. Di Carlo, "Plasmon polaritons in the near infrared on fluorine doped tin oxide films," *Opt. Exp.*, vol. 17, pp. 10155–10167, 2009.
[36] Y. B. Zheng, B. K. Juluri, X. Mao, T. R. Walker, and T. J. Huang, "Systematic investigation of localized surface plasmon resonance of long-range ordered Au nanodisk arrays," *J. Appl. Phys.*, vol. 103, pp. 014308-1–014308-9, 2008.
[37] T. Rindzevicius, Y. Alaverdyan, M. Käll, W. A. Murray, and W. L. Barnes, "Long-range refractive index sensing using plasmonic nanostructures," *J. Phys. Chem. C*, vol. 111, pp. 11806–11810, 2007.
[38] U. Kreibig and M. Vollmer, *Optical Properties of Metal Clusters*. New York, USA: Springer, 1995.
[39] C. F. Bohren and D. R. Huffman, *Absorption and Scattering of Light by Small Particles*. New York, USA: Wiley-VCH, 2008.
[40] U. Guler and R. Turan, "Effect of particle properties and light polarization on the plasmonic resonances in metallic nanoparticles," *Opt. Exp.*, vol. 18, pp. 17322–17338, 2010.
[41] C. Langhammer, M. Schwind, B. Kasemo, and I. Zoric, "Localized surface plasmon resonances in aluminum nanodisks," *Nano Lett.*, vol. 8, pp. 1461–1471, 2008.
[42] C. Langhammer, Z. Yuan, I. Zoric, and B. Kasemo, "Plasmonic properties of supported Pt and Pd nanostructures," *Nano Lett.*, vol. 6, pp. 833–838, 2006.
[43] B. Y. Oh, M. C. Jeong, D. S. Kim, W. Lee, and J. M. Myoung, "Post-annealing of Al-doped ZnO films in hydrogen atmosphere," *J. Crystal Growth*, vol. 281, pp. 475–480, 2005.
[44] K. Yim, H. Kim, and C. Lee, "Effects of annealing on structure, resistivity and transmittance of Ga doped ZnO films," *Mater. Sci. Technol.*, vol. 23, pp. 108–112, 2007.
[45] G. Gonçalves, E. Elangovan, P. Barquinha, L. Pereira, R. Martins, and E. Fortunato, "Influence of post-annealing temperature on the properties exhibited by ITO, IZO and GZO thin films," *Thin Solid Films*, vol. 515, pp. 8562–8566, 2007.
[46] K. P. Chen, V. P. Drachev, J. D. Borneman, A. V. Kildishev, and V. M. Shalaev, "Drude relaxation rate in grained gold nanoantennas," *Nano Lett.*, vol. 10, pp. 916–922, 2010.

**Jongbum Kim** received the B.E. degree in electrical and computer engineering from Korea University, Seoul, Korea, in 2007. He is currently working toward the Ph.D. degree in the Department of Electrical Engineering, Purdue University, West Lafayette, IN, USA.

His research interests include fabrication of devices for plasmonics and metamaterials.

**Gururaj V. Naik** received the Bachelor degree in electronics and communication engineering from Visvesvaraya Technological University, Belgaum, India, in 2006, and the M.E. degree in microelectronics from the Indian Institute of Science, Bangalore, India, in 2008, with Gold Medal. Since January 2009, he has been working toward the Ph.D. degree in nanophotonics at Purdue University, West Lafayette, IN, USA.

His research interests include materials and devices for plasmonics and metamaterials.

**Naresh K. Emani** (M'10) received the M.Sc. degree in physics from Sri Sathya Sai University, Puttaparthi, India, in 2005, and the M.Tech. degree in electrical engineering from the Indian Institute of Technology Bombay, Mumbai, India, in 2007. He is currently working toward the Ph.D. degree in electrical engineering at Purdue University, West Lafayette, IN, USA.

From 2007 to 2009, he worked on bias temperature instability in MOSFETs at Taiwan Semiconductor Manufacturing Company, Taiwan. His current research interests include simulation and fabrication of tunable Nanophotonic devices and Metamaterials.

**Urcan Guler** received the B.S. and M.S. degrees in physics from Middle East Technical University, Ankara, Turkey, in 2007 and 2009, respectively. He is currently working toward the Ph.D. degree in the Department of Electrical Engineering, Purdue University, West Lafayette, IN, USA.

His research interests include modelling and fabrication of plasmonic structures.

**Alexandra Boltasseva** (M'09) received the Ph.D. degree in electrical engineering from the Technical University of Denmark (DTU), Lyngby, Denmark, in 2004.

She is currently an Assistant Professor at the School of Electrical and Computer Engineering and Birck Nanotechnology Center, Purdue University, West Lafayette, IN, USA, and an adjunct Associate Professor at DTU. She specializes in nanophotonics, nanofabrication, plasmonics, and metamaterials.

Dr. Boltasseva received the Young Elite-Researcher Award from the Danish Council for Independent Research in 2008, Young Researcher Award in Advanced Optical Technologies from the University of Erlangen-Nuremberg in Germany in 2009, and the Technology Review Top Young Innovator Award TR35 in 2011. She is a Topical Editor for *Optics Letters* and *Journal of Optics*, a Senior Member of the Optical Society of America, and a member of the International Society for Optical Engineers and the American Materials Research Society.